Available online at www.sciencedirect.com

SCIENCE DIRECT®

Graphical Models 67 (2005) 549–564

Graphical Models

www.elsevier.com/locate/gmod

Rendering cartoon-style motion cues in post-production video

J.P. Collomosse [a,*], D. Rowntree [b], P.M. Hall [a]

[a] *Department of Computer Science, University of Bath, Claverton Down, Bath, England, UK*
[b] *Nanomation Ltd., 6 Windmill Street, London, England, UK*

Received 17 October 2003; accepted 7 December 2004
Available online 13 April 2005
Communicated by Peter Hall and Brain Barsky

Abstract

The contribution of this paper is a novel non-photorealistic rendering (NPR) system capable of rendering motion within a video sequence in artistic styles. A variety of cartoon-style motion cues may be inserted into a video sequence, including augmentation cues (such as streak lines, ghosting, or blurring) and deformation cues (such as squash and stretch or drag effects). Users may select from the gamut of available styles by setting parameters which influence the placement and appearance of motion cues. Our system draws upon techniques from both the vision and the graphics communities to analyse and render motion and is entirely automatic, aside from minimal user interaction to bootstrap a feature tracker. We demonstrate successful application of our system to a variety of subjects with complexities ranging from simple oscillatory to articulated motion, under both static and moving camera conditions with occlusion present.
© 2005 Elsevier Inc. All rights reserved.

Keywords: Video paintbox; Motion cues; NPR; Cartoon rendering

* Corresponding author.
E-mail addresses: jpc@cs.bath.ac.uk (J.P. Collomosse), david@nanomation.co.uk (D. Rowntree), pmh@cs.bath.ac.uk (P.M. Hall).

1524-0703/$ - see front matter © 2005 Elsevier Inc. All rights reserved.
doi:10.1016/j.gmod.2004.12.002

1. Introduction

This paper presents a novel non-photorealistic rendering (NPR) system capable of rendering motion within a 2D image sequence in artistic styles. The user may stylise the rendering through a parameterised framework encompassing a diverse gamut of motion cues commonly used in animation; augmentation cues such as streak lines, ghosting, and blurring are available, as are deformation cues such as the squash and stretch techniques used to emphasise motion in cartoons. The algorithm draws upon techniques from both the vision and the graphics communities to analyse and render motion. Aside from minimal interaction when bootstrapping a feature tracker, the system is entirely automatic.

Our work is motivated by a desire to render 2D image sequences in cartoon-like styles, a problem that decomposes into two separable sub-goals: (1) producing temporally coherent shading effects in the video; (2) emphasising motion in the image sequence. Whilst we do address the former issue, this paper is primarily concerned with the latter issue of visually depicting motion through artistic rendering. To the best of our knowledge we believe that artistic rendering of motion within a video sequence is a novel contribution to NPR, and one that implies interesting new application areas for Computer Vision.

The majority of research in non-photorealistic animation focuses upon the synthesis of 2D artistically rendered sequences from 3D geometries [1,2]. Some progress has been made in processing 2D video sequences into non-photorealistic styles, for example the animated painterly effects proposed by Litwinowicz [3], and later Hertzmann [4]. Such algorithms focus primarily upon the task of extending static NPR techniques to moving video whilst maintaining temporal coherence (avoiding flickering) in the image sequence. Whilst such methods seek to mitigate against the effects of motion for the purposes of coherence, the literature is relatively sparse concerning the emphasising and rendering of motion within the image sequence itself.

In an early paper [5], Lasseter highlights many of the motion emphasis techniques commonly used by animators for the benefit of the computer graphics community, though presents no algorithmic solutions. Streak lines, anticipation, and deformation for motion emphasis are discussed. Recent work addresses one of these techniques by applying a squash and stretch effect to spheres and cylinders in object space prior to ray-tracing [6]. Strothotte et al. [7], after Hsu et al. [8], also identify depiction of motion as important, though the former are concerned primarily with the effect of motion cues on temporal perception. In both studies streak lines are generated via user-interactive processes. Earlier work by the authors renders motion within an image sequence by composing salient features to produce paintings reminiscent of Cubist art [9].

Animators have evolved various ways of emphasising characteristics of a moving object (Fig. 1). Streak lines are commonly used to emphasise motion, and typically follow the movement of the tip of the object through space. The artist can use additional 'ghosting' lines which indicate the trailing edge of the object as it moves along the streak lines. Ghosting lines are usually perpendicular to streak lines. Deformation is often used to emphasise motion, and a popular technique is squash and

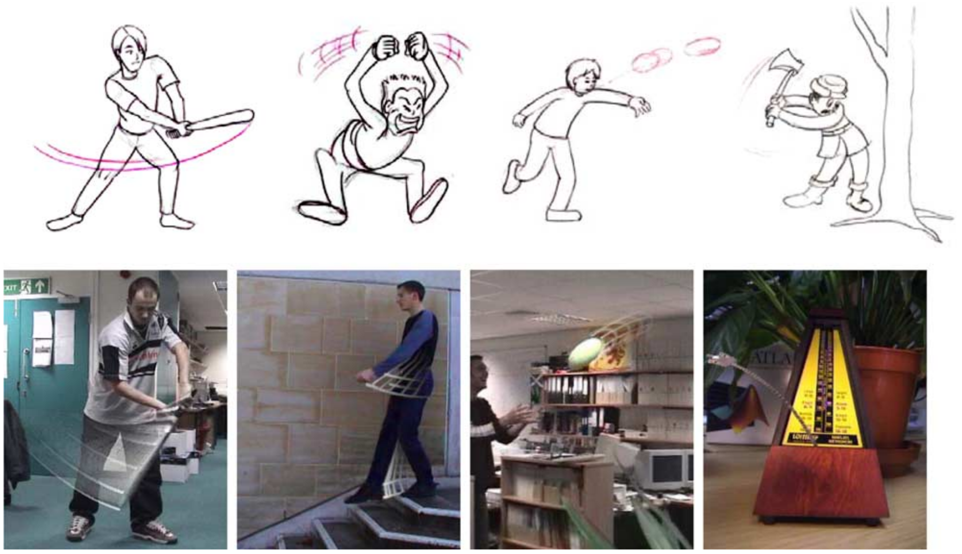

Fig. 1. Examples of motion cues used in traditional animation (above) and the corresponding cues inserted into a video sequence by our system (below). From left to right: two examples of streak line augmentation cues, the latter with ghosting lines. Two examples of deformation cues; squash and stretch and suggestion of inertia through deformation.

stretch in which a body is stretched tangential to its trajectory, whilst conserving area [5]. Other deformations can be used to emphasise an object's inertia; a golf club or pendulum may bend along the shaft to show the end is heavy and the accelerating force is having trouble moving it. The magnitude of deformation is a function of motion parameters such as tangential speed, and of the modelled rigidity of the object. In this paper, we process real video to introduce these motion cues; examples are given in Fig. 1.

An attempt to automatically render motion cues presents the following challenges:

(1) Motion cues tend to emphasise fast, large-scale feature motions, the filming of which often requires the camera to move. Features may also become occluded during motion. How shall we track features through a video sequence in these circumstances, and what constraints must we impose to make the tracking problem tractable?
(2) How will motion cues be generated and attached to tracked features? How will such cues adapt to variations in velocity and acceleration? How will motion cues be embedded coherently in the existing image sequence?
(3) How can we render the final scene to produce coherent artistic shading styles?

The first point falls within the bounds of Computer Vision, the latter two are primarily Computer Graphics issues.

The remainder of the paper is organised as follows. In Section 2, we give an overview of the system. In Section 3, we discuss the vision algorithms for camera motion correction and tracking. In Section 4, we describe the algorithms for generating motion cues and inserting them into video. We conclude in Section 5 with a discussion of future work.

2. Overview of the system

We now describe the major components of the system, leaving detailed explanation to subsequent sections of the paper. The system has two major components: the Computer Vision component which is responsible for tracking motion of features (e.g., arm, leg, bat or ball), camera motion compensation, and depth ordering of features; and the Computer Graphics component, responsible for the generation of motion cues, and their rendering at the correct depth. We wish for minimal user interaction with the Computer Vision component, which must be robust and general; currently users draw polygons in a single frame to identify features which are then tracked automatically. In contrast, the user is given control over the graphics component via a set of parameters which influence the style in which the motion cues are synthesised.

3. The computer vision component

The Computer Vision component is responsible for the tracking of features over the video sequence. A camera motion compensated version of the sequence is first generated, thereby ensuring that camera motion does not influence the observed trajectories. Features are then tracked over the sequence using standard techniques. By analysing occlusion during tracking we determine a relative depth ordering of features, later used in the rendering stage to insert motion cues at the correct scene depth.

We compensate for camera motion using a robust motion estimation technique proposed by Torr [10]. Harris interest points [11] are identified in adjacent video frames, and RANSAC [12] use to produce an initial estimate of the homography between frames. This estimate is then refined using a Levenburg–Marquadt iterative search [13]. Frames are projected via their homographies to produce a motion compensated sequence in which the tracking of features is subsequently performed.

3.1. Tracking features over the compensated sequence

The general problem of tracking remains unsolved in Computer Vision and, like others, we now introduce constraints on the source video in order to make the problem tractable. Users identify features by drawing polygons, which are "shrink wrapped" to the feature's edge contour [14]. We assume contour motion may be modelled by a linear conformal affine transform (LCAT) in the image plane, which has four parameters (scale, orientation, and spatial position). Variation of these parameters is assumed to well approximate a second order motion equation over short time intervals.

The LCAT is a degenerate form of the affine transform consisting of a uniform scale s, orientation θ, and a translation $(u, v)^T$. In homogeneous coordinates we have a product of matrices

$$\underline{\underline{M}}(s, \theta, u, v) = \underline{\underline{T}}(u, v)\underline{\underline{R}}(\theta)\underline{\underline{S}}(s) \tag{1}$$

A feature, F, comprises a set of points whose position varies in time; we denote a point in the tth frame by the column vector $\underline{x}_t = (x, y)_t^T$. In general these points are not pixel locations, and so we use bilinear interpolation to associate a colour value, $I(\underline{x}_t)$ with the point. The colour value comprises the hue and saturation components of the HSV colour model; we wish to ignore variations in luminance to mitigate against errors introduced by lighting changes. Although the LCAT can be derived from two point correspondences we wish to be resilient to outliers, and therefore seek the LCAT $\widehat{\underline{\underline{M}}_{tt'}}$ which minimises $E[.]$

$$E[\underline{\underline{M}}_{tt'}] = \frac{1}{|F|} \sum_{i=1}^{|F|} |I(\underline{x}_{t'}^i) - I(\underline{\underline{M}}_{tt'} \underline{x}_t^i)|^2, \tag{2}$$

where the tt' subscript denotes the matrix transform from frame t to t'. In a similar manner to camera motion correction, the transformation $\underline{\underline{M}}_{tt'}$ is initially estimated by RANSAC, and then refined by Levenburg–Marquadt search.

By default, several well distributed interest points are identified automatically using the Harris [11] detector (see sequences *CRICKET*, *METRONOME*). In some cases a distinctively coloured feature itself may be used as a marker (see *VOLLEY*, Fig. 2). In more complex cases where point correspondences for tracking can not be found (perhaps due to signal flatness, small feature area, or similarity between

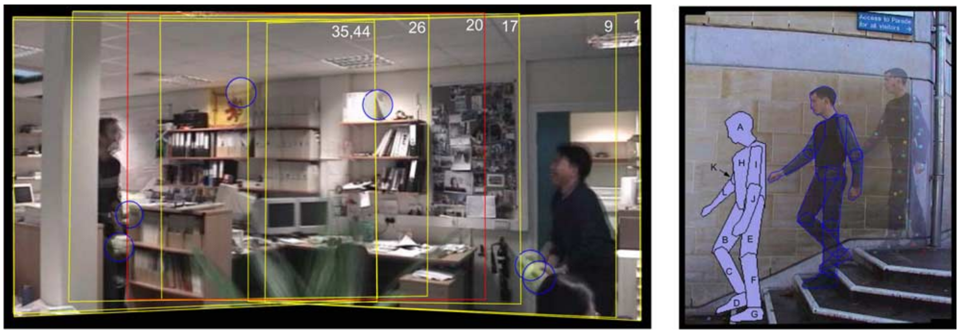

Fig. 2. Left: The camera compensated *VOLLEY* sequence sampled at regular time intervals. The camera view-port at each instant is outlined in yellow, the tracked feature in blue. Right: *STAIRS* sequence. (Top) markers are required to track this more complex subject but are later removed automatically (middle). Recovery of relative depth ordering permits compositing of features in the correct order (bottom); labels A–K correspond to the graph of Fig. 3. (For interpretation of the references to color in this figure legend, the reader is referred to the web version of this paper.)

closely neighbouring features), distinctively coloured markers may be physically attached to the subject and later removed digitally (see *STAIRS*, Fig. 2). In these cases the Harris interest points are substituted for points generated by analysis of the colour distribution in a frame.

So far we have overlooked noise and occlusion. The 'best' $\underline{\underline{M}}_{tt'}$ estimate may be considered to be arbitrary in the case of total occlusion, and exact in the case of no noise or occlusion. The likelihood L_t of the feature being *unoccluded* at any time t may be written as a function of detected pixel error $L_t = \exp(-\lambda E_{[\underline{\underline{M}}_{tt'}]})$; λ is the reciprocal of the average time an object is unoccluded. At each frame t we pass the estimated LCAT $\underline{\underline{M}}_{tt'}$, and the confidence in that estimate, L_t, through a Kalman filter to obtain our optimal estimate for the LCAT. The Kalman filter state describes the second order motion equation in the 4D parameter space of the LCAT, trained over the immediate history of contour motion. We threshold L_t at 0.5 to decide whether an object is occluded in a given frame, and interpolate the LCAT from unoccluded neighbours in these cases.

The ability of the algorithm to re-establish tracking following occlusion has been found sufficiently robust for our needs, providing occluded motion approximately follows the second order model estimated by the Kalman filter. However the predicted LCAT during occlusion is often inaccurate. We refine the tracked motion by deciding at which time intervals a feature is occluded and interpolating between the parameters of known LCATs immediately before and after occlusion. Knowledge of the correct positions of features during occlusion is important when rendering as although a feature may not be visible, any attached motion cues may be. Occlusion is also used to determine relative feature depth.

3.2. Recovering relative depth ordering of features

We now determine a partial depth ordering for tracked features, based on their mutual occlusion over time. The objective is to assign an integer value to each feature corresponding to its relative depth from the camera. We introduce additional assumptions at this stage: (1) the physical ordering of tracked features cannot change over time (potential relaxation of this assumption is discussed in Section 5); (2) a tracked feature can not be both in front and behind another tracked feature; and (3) lengthly spells of occlusion occur due to tracked features inter-occluding.

For each instance of feature occlusion we determine which interest points were occluded by computing a difference image between tracked and original feature bitmaps. A containment test is performed to determine if occluded points lie with the bounding contour of any other tracked features; if this is true for exactly one feature, then the occlusion was caused by that feature. We represent these inter-feature relationships as a directed graph, which we construct by gathering evidence for occlusion over the whole sequence. Formally, we have a graph of nodes $G_{1...n}$ corresponding uniquely with the set of tracked features, where $G_i \mapsto G_j$ implies that feature G_i occludes G_j (Fig. 3). Each graph edge is assigned a weight; a count of how many times the respective occlusion is detected.

This graph has several important properties. First, the graph *should be* acyclic since cycles represent planar configurations which cannot occur unless our previous

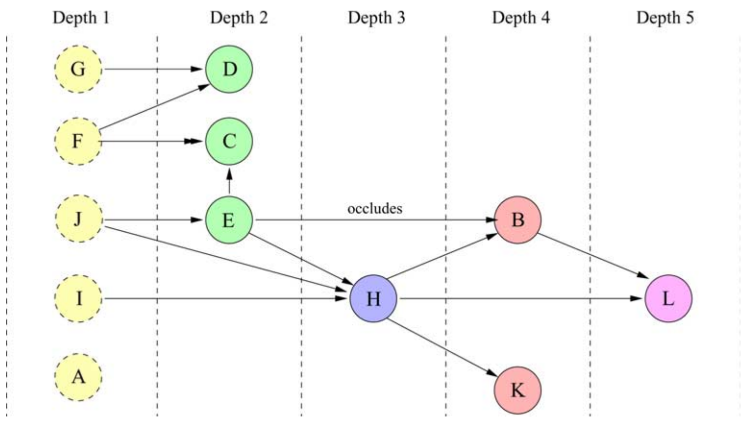

Fig. 3. An occlusion graph constructed over 150 frames of the *STAIRS* sequence, node letters correspond with Fig. 2. Dotted lines indicate unoccluded nodes.

assumptions are violated or, rarely, noise has cause false occlusion. Second, groups of polygons may not interact via occlusion, thus the resulting graph may not be connected (a forest). Third, at least one 'unoccluded node' G_m must exist per connected graph such that $\forall G_i = 1 \ldots n \neg \exists G_i \mapsto G_m$.

First, we verify that the graph is indeed acyclic. If not, cycles are broken by removing the cycle's edge of least weight. This removes sporadic occlusions which can appear due to noise. We now assign an integer *depth code* to each node in the graph; smaller values represent features closer to the camera. The value assigned to a particular node corresponds to the maximum of the hop count of the longest path from any unoccluded node to that node (Fig. 3). By definition features within disconnected graphs do not occlude each other, thus it is not possible to determine a consistent ordering over all connected graphs using occlusion alone. However, since these data are required later only to composite features in the correct order, such consistency is superfluous to our needs.

4. The computer graphics component

The graphics component composits cells to create each frame of the animation. Each feature has two cells associated with it, one for *augmentation cues* such as streak lines, the other for *deformation cues* such as squash and stretch. The cells are composited according to the depth ordering of features, from the furthest to the nearest; for a given feature, deformation cells are always in front of augmentation cells.

4.1. Motion cues by augmentation

Augmentation cues such as streak lines and ghosting, are common in traditional animation (Fig. 1). Streak lines can be produced on a per frame basis by attaching lines to a feature's trailing edge, tangential to the direction of motion [8]. Such an approach is only suitable for visualising instantaneous motion, produces only straight streak lines, and is highly susceptible to noise. In contrast animators tend to sketch elegant, long curved streaks which emphasise motion historically. For the same reasons, optical flow cannot be used to create streak lines.

Streak line placement is a non-trivial problem: they are not point trajectories, features tend to move in a piecewise-smooth fashion, and we must carefully place streak lines on features. To produce streak lines we generate *correspondence trails* over the trailing edge of a feature as it moves, we then segment trails into smooth sections, which we filter to maximise some objective criteria. We finally render the chosen sections in an artistic style.

We sample the feature boundary at regular intervals, identifying a point as being on the trailing edge if the dot product of its motion vector with the external normal to the boundary is negative. Establishing correspondence between trailing edges is difficult because point ordering can vary from frame to frame, as well as shape (and even connectivity). The full LCAT determined during tracking cannot be used, as this establishes point trajectories (which we have observed are not streak lines); we wish to establish correspondence between feature silhouettes.

We establish correspondence trails by computing the instantaneous tangential velocity of a feature's centroid $\underline{\mu}$. A translation and rotation is computed to map the normalised motion vector from $\underline{\mu}$ at time t to time t'. Any scaling of the feature is performed using the scale parameter of the LCAT determined during tracking. Points on the trailing edge at time t are now translated, rotated, and scaled. Correspondence is established between these transformed points at time t, and their nearest neighbours at time t', this forms an link in a correspondence trail. This method gives independence on point ordering, and allows the geometry of the trailing edge to vary over time, as required.

Animators tend to draw streak lines over smooth sections of motion. Therefore, the correspondence trails are now segmented into smooth sections, delimited by sharp changes in trajectory. Such motion is usually caused by rapid translational, rotary or projectile motion in a scene, resulting in simple linear or curved trajectories. We have therefore chosen to model these trajectories using a subset of conics; elliptic curve fragments, parabolic curve fragments (which permit linear forms as a degeneracy).

We use a greedy algorithm to fit curves: (1) begin at the start of the correspondence trail; (2) iterate forward capturing points and fitting elliptical [15] and parabolic curves along the way using least-squares; and (3) when no curve fits sufficiently well (below a threshold), or average velocity falls too low, the smooth section is terminated and the best fitting curve used as a model for that section.

We fit piecewise smooth models to every correspondence trail, as just described. This results in a set of smooth sections, each with a pair of attributes: (1) a function $G(s)$ where s is an arc-length parameterisation of the spatial trajectory of the fitted curve $s = [0,1]$; (2) a lookup table $g(.)$ mapping from an absolute time index t to the arc-length parameter, i.e., $s = g(t)$, thus recording velocity along the spatial path $\underline{G}(s)$. The inverse lookup function $g'(.)$ is also available. Clearly the curve exists only for a specific time period $[g'(0), g'(1)]$; we call this interval the duration of the curve.

The association between each smooth section and its data points is maintained. These data points are used to filter the set of smooth sections to produce a subset σ of manageable size, which contains optimal paths along which streak lines will be drawn.

Our filtering selects curves based on heuristics derived from the practise of traditional animators who favour placement of streak lines on sites of high curvature and on a feature's convex hull. Long streak lines and streak lines associated with rapid motion are also preferred, but close proximity to other co-existing streak lines is discouraged. We select streak line curves, on each iteration i adding a new element to σ (initially empty) to maximise the recursive function $H(.)$:

$$\begin{aligned} H(0) &= 0, \\ H(i+1) &= H(i) + (\alpha v(x) + \beta L(x) - \gamma D(x) - \delta\omega(x,\sigma;w) + \zeta\rho(x)), \end{aligned} \tag{3}$$

where x is the set of points associated with a smooth section. $L(x)$ is the length of a smooth section, $v(x)$ is the "mean velocity" defined as $L(x)/t(x)$ in which $t(x)$ is the duration of x. $\rho(x)$ is the mean curvature of feature boundary at points in x. $D(x)$ is the mean shortest distance of points in x from the convex hull of the feature. $\omega(x,\sigma;w)$ measures the maximal spatio-temporal overlap between x and the set of streak lines chosen on previous iterations. From each curve we choose points which co-exist in time, and plot the curves with width w returning the intersected area. Constant w is user defined, as are the constant weights α, β, γ, δ, and ζ; these give artistic control over the streak line placement (see Fig. 4). Iteration stops when the additive measure falls below a lower bound.

We are now in a position to synthesise two common forms of augmentation cue; streak lines and ghosting lines—both of which are spatio-temporal in nature. A streak line is made visible at some absolute time t and exists for a duration of time Δ. The streak line is rendered by drawing a sequence of discs along the smooth section with which it is associated, starting at spatial location $\underline{G}(g(t))$ and ending at

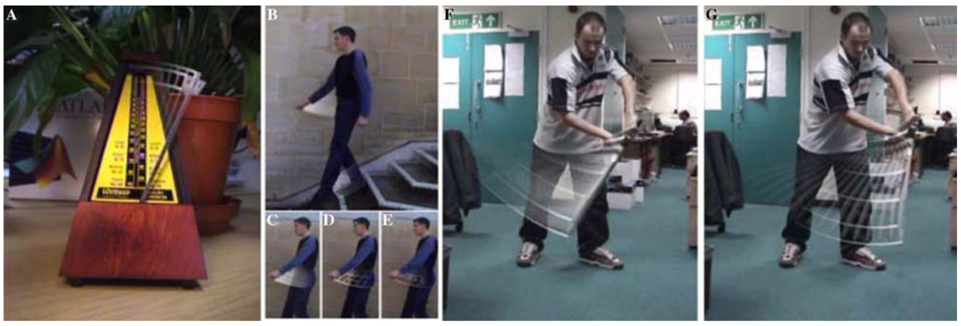

Fig. 4. A selection from the gamut of streak and ghosting line styles available: ghosting lines may be densely sampled to emulate motion blur effects (B, C, and F) or more sparsely for traditional ghosting (A and D). The feature itself may be ghosted, rather than the trailing edge, to produce Futurist-like echoes (E and G). Varying the overlap constant w influences spacing of streak lines (B and F). The decay parameters of streak and ghosting lines may be set independently (A).

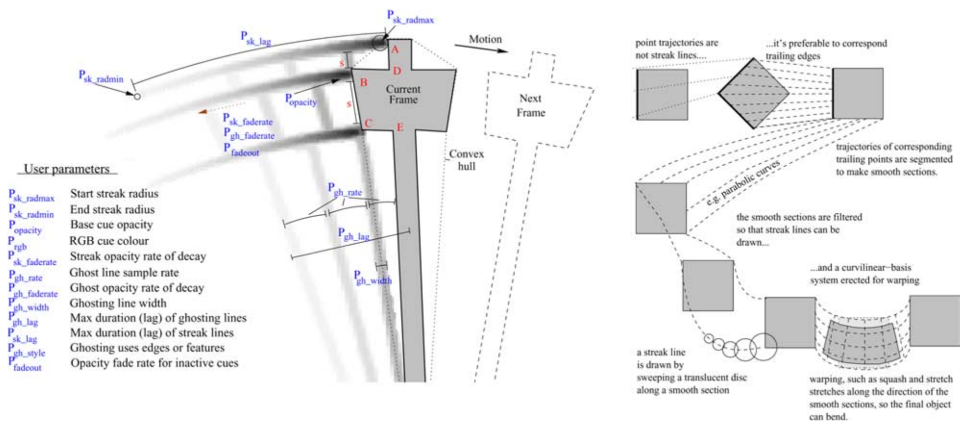
P_{sk_radmax}
P_{sk_lag}
P_{sk_radmin}
Motion
A
D
B
Current Frame
$P_{opacity}$
s
s
C
E
$P_{sk\_faderate}$
$P_{gh\_faderate}$
$P_{fadeout}$
Next Frame
Convex hull
P_{gh_rate}
P_{gh_lag}
P_{gh_width}
point trajectories are not streak lines....
...it's preferable to correspond trailing edges
trajectories of corresponding trailing points are segmented to make smooth sections.
e.g. parabolic curves
the smooth sections are filtered so that streak lines can be drawn...
...and a curvilinear–basis system erected for warping
a streak line is drawn by sweeping a translucent disc along a smooth section
warping, such as squash and stretch stretches along the direction of the smooth sections, so the final object can bend.

User parameters

P_{sk_radmax}	Start streak radius
P_{sk_radmin}	End streak radius
$P_{opacity}$	Base cue opacity
P_{rgb}	RGB cue colour
$P_{sk\_faderate}$	Streak opacity rate of decay
P_{gh_rate}	Ghost line sample rate
$P_{gh\_faderate}$	Ghost opacity rate of decay
P_{gh_width}	Ghosting line width
P_{gh_lag}	Max duration (lag) of ghosting lines
P_{sk_lag}	Max duration (lag) of streak lines
P_{gh_style}	Ghosting uses edges or features
$P_{fadeout}$	Opacity fade rate for inactive cues

Fig. 5. Left: User parameters used, in conjunction with weights of Eq. (3), to influence augmentation cue placement. Right: Summarising the generation of motion cues in our framework.

$\underset{\dots}{G}(g(\arg\max(g'(0), t - \Delta)))$. The streak line is rendered by sweeping a translucent disc along the smooth section (backwards in time) which grows smaller and more transparent over time. These decays are under user control. Secondary streak lines may be generated at small spatio-temporal offsets to produce sketchy or turbulent effects.

Ghosting lines depict the position of a feature's trailing edge along the path of the streak line, and are useful in visualising velocity changes over the course of the streak. Ghosting lines are rendered by sampling the trailing edge at regular time intervals as the streak line is rendered, interpolating if required. The opacity of ghosting lines is not only a function of time (as with streak lines) but also a function speed relative to other points on the trailing edge; this ensures only fast moving regions of edge are ghosted. Users may control the sampling rate, line thickness, and decay parameters to stylise the appearance of the ghosting lines (Fig. 5).

4.2. Motion cues by deformation

Our framework offers the facility to emulate effects such as 'squash and stretch,' or to suggest inertia or drag through deformation. Features are cut from the current video frame, and motion dependent warping functions applied to render the deformation cue cell for each feature.

Deformations are performed by forming a curvilinear space, the basis of which is defined by the local trajectory of the feature centroid, and lines normal to this curve; this trajectory has exactly the same properties as any smooth section. A local time-window selects a section of the centroid trajectory, and this window moves with the object. The instantaneous spatial width of this window is proportional to instantaneous centroid velocity. At each instant, t we use the centroid trajectory to establish a curvilinear basis frame. First, we compute an arc-length parameterisation of the trajectory: $\underline{\mu}(r)$ in which $r = \int_t^{t'} \underline{\dot{\mu}(t)}\,\mathrm{d}t$, note $t' < t$ gives negative displacements. Next we develop an ordinate at an arc-length distance r from the instant; the unit vector $\underline{n}(r)$ perpendicular to $\underline{\dot{\mu}(t)}$. Thus, at each instant t we can specify a point in the world-frame using two coordinates, r and s

$$\underline{x}_t(r,s) = \mu(r) + s\underline{n}(r). \tag{4}$$

We can write this more compactly as $\underline{x}_t(\underline{r}) = \underline{C}(\underline{r})$, where $\underline{r} = [r,s]^T$, and maintain the inverse function $\underline{r}_t(\underline{x}) = \underline{C}^{-1}(\underline{x})$ via a look-up table. This mapping, and its inverse, comprise one example of a *deformation basis*.

The above analysis holds for most points on the centroid trajectory. It breaks down at *collision points*, because there is a discontinuity in velocity. We define a collision point as a point on a trajectory whose location cannot be satisfactorily predicted by a second order motion equation (constructed with a Kalman filter). This definition discriminates between G^1 discontinuities in trajectory which are formed by, say, simple harmonic motion, and true collisions which are C^1 discontinuous (see Fig. 6).

At a collision point we establish an orthonormal basis set aligned with the observed collision plane. We assume the angle of incidence and reflection are equal, and hence the unit vector which bisects this angle is taken to be the ordinate. The abscissa lies in the collision plane. We define this new basis set as an additional instance of a deformation basis, and write the mapping to and from the world frame using notation consistent with the curvilinear basis. In addition, we compute the *impact parameter* of the collision, which we define as the distance from the object's centroid to its boundary, in the direction of the negative ordinate. Note we compensate for temporal sampling around the true collision instant by intersecting extrapolated impact and rebound trajectories (Fig. 6).

An animated object is, in general, a deformed version of the original. Squash and stretch tangential to instantaneous motion leads to visually unattractive results; it is better to not only squash and stretch, but also to bend the object along the arc of its centroid trajectory. Let $\underline{x}(t)$ be any point in the object. We transform this point with respect to a single deformation basis into a new point $\underline{y}(t)$, given by

$$\underline{y}(t) = C(A_t[C^{-1}(\underline{x}(t))]), \tag{5}$$

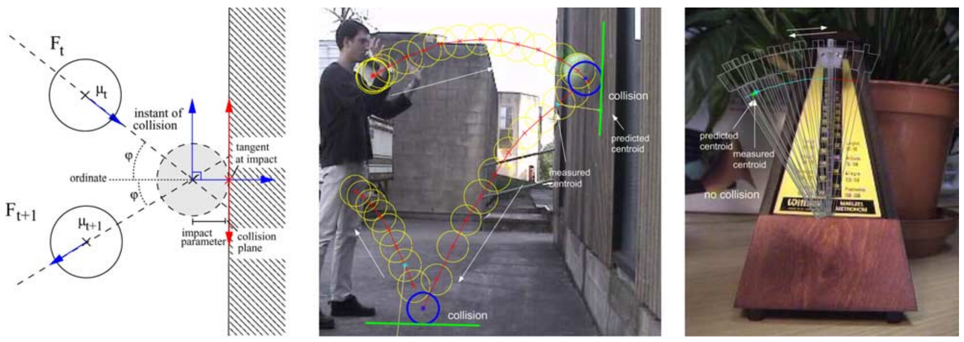

Fig. 6. Collision geometry (left); bounces are detected as collisions (middle); whilst the simple harmonic motion of the metronome is not (right).

where $A_t[.]$ is some deformation. In the case of squash and stretch the deformation is an area-preserving differential scale that depends on instantaneous speed $|\underline{\dot{\mu}}(t)|$ (see Fig. 7):

$$A = \begin{bmatrix} k & 0 \\ 0 & \frac{1}{k} \end{bmatrix}, \tag{6}$$

$$k = 1 + \frac{K}{2}\left(1 - \cos\left(\pi\frac{v^2+1}{2}\right)\right),$$

$$v = \begin{cases} 0 & \text{if } |\underline{\dot{\mu}}| < V_{\min}, \\ 1 & \text{if } |\underline{\dot{\mu}}| \geqslant V_{\max}, \\ (|\dot{\mu}| - V_{\min})/(V_{\max} - V_{\min}) & \text{otherwise.} \end{cases} \tag{7}$$

Around collision points we need to squash and stretch the other way around—so that the object compresses on impact. We linearly interpolate between the deformation caused by a "standard" deformation basis with that caused by a "collision" deformation basis. Suppose $\underline{p}(t) \mapsto \underline{q}(t)$ and $\underline{p}(t) \mapsto \underline{q}'(t)$, respectively, then

$$\underline{r}(t) = f(d)\underline{q}(t) + (1 - f(d))\underline{q}'(t), \tag{8}$$

where $f(d) = \sin(\frac{\pi}{2}\text{argmin}(1, d/(sD))$ in which D is the impact parameter of the collision, and s is a user parameter which controls the spatial extent over which collision influences the deformation. As a note, the mapping to $\underline{q}'(t)$ not only has to scale the

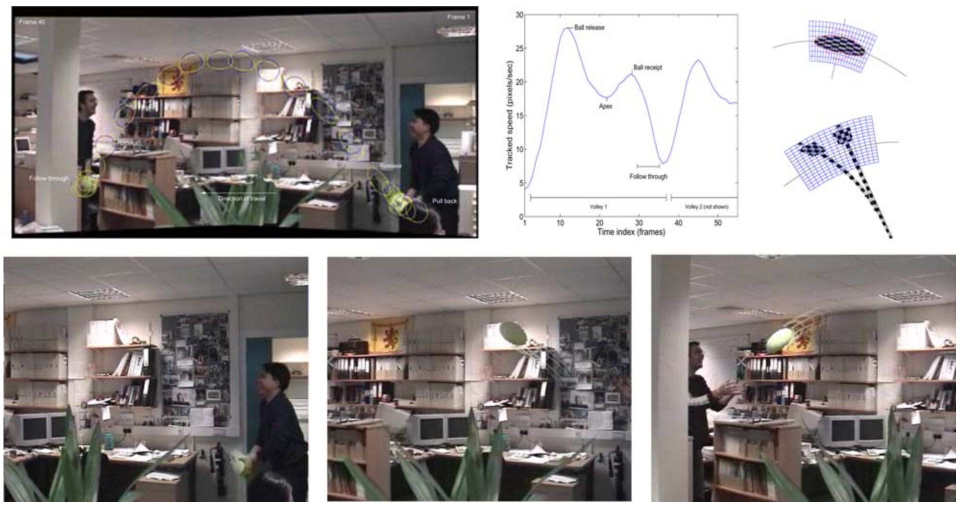

Fig. 7. Top left: Illustrating the squash and stretch effect; eccentricity varies as a function of tangential speed. Bottom: Frames from the *VOLLEY* sequence exhibiting squash and stretch. Observe the system handles both large scale camera motion, and lighting variation local to the ball. Top right: Curvilinear space used to deform features in *VOLLEY* and *METRONOME*.

object but shift it toward the impact point, so that the edge of the deformed object touches the collision plane.

Non-linear deformations are also possible, and these can be used to create bending effects. We can form warping functions which depend on each point's velocity and acceleration as well as its position. We write $x' = C(A_t[C^{-1}(\underline{x}), \dot{\underline{x}}, \ddot{\underline{x}}])$, where A is a functional used, for example, to suggest increased drag or inertia. A typical functional operates on each component of $\underline{r} = (r_1, r_2)^T$ independently; to create effects suggesting drag we use:

$$r_1 \leftarrow r_1 - F\left(\frac{2}{\pi}\text{atan}(|\dot{\underline{x}}_i|)\right)^P \text{sign}(\dot{\underline{x}}_i), \tag{9}$$

where F is a function of suggested mass and P influences the apparent rigidity of the object. By substituting acceleration for velocity, and adding rather than subtracting from r_1 we can emphasise inertia of the feature (see Fig. 8).

Finally, we ensure visual consistency by deforming not only features, but also their associated augmentation cue cells containing streak lines or ghost lines.

4.3. Rendering in the presence of occlusion

In any real video a tracked feature may become occluded by other elements of the scene. Naïvely, all pixels inside the bounding contour of a feature will be included in that feature and so are subject to deformation. Consequently, it is easy to warp parts of occluding objects; we now explain how to avoid such unwelcome artifacts.

We identify pixels as belonging to an occluding object by forming a difference image (using the hue and saturation components in HSV space) between the feature region in the current frame and the feature itself. This yields a template of occluding pixels which can be re-textured by sampling from feature regions in neighbouring unoccluded frames. The unoccluded feature is thus reconstructed, and after deformation occluding pixels may be recomposited to give the illusion of the ball passing 'behind' occluding objects (Fig. 9).

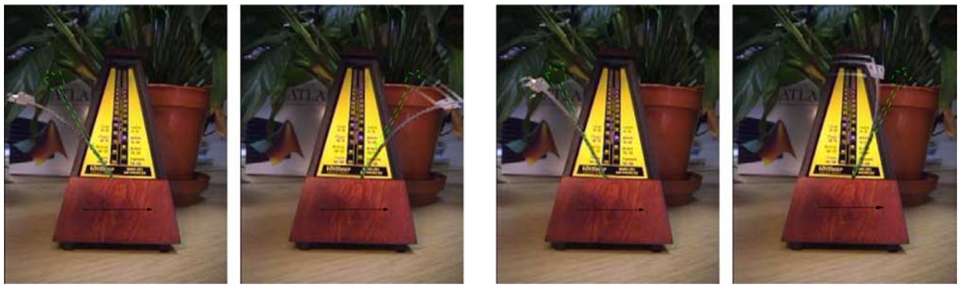

Fig. 8. Frames from *METRONOME* suggesting inertia (left) and drag (right) effects through deformation, original feature outline in green. (For interpretation of the references to color in this figure legend, the reader is referred to the web version of this paper.)

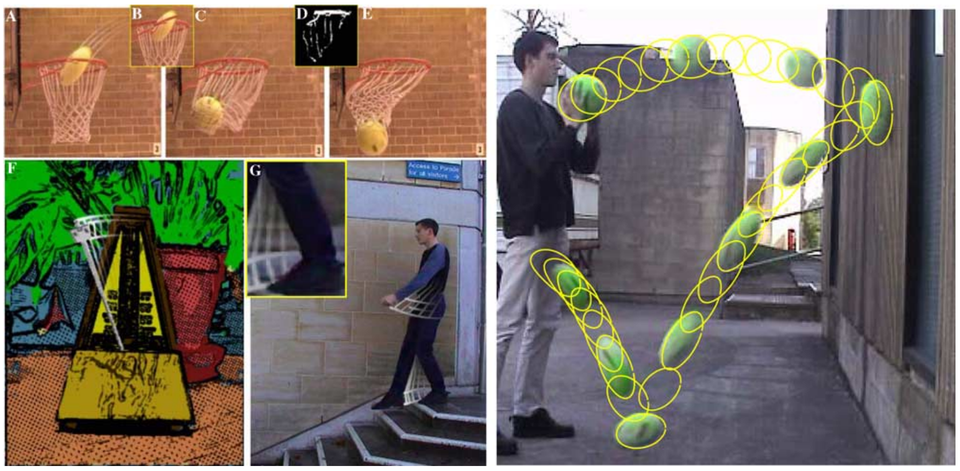

Fig. 9. Above: three frames from *BASKETBALL*, demonstrating occlusion handling. The system fails when the netting moves erratically after impact, causing the buffer to empty and streak lines to be drawn in front of the netting (E). Below left: A coherent cartoon effect created by applying Q-maps to cells [16]; Below middle: Streak lines are inserted at the correct scene depth; cues attached to the far leg pass behind the near leg. Right: Time lapse image of *BOUNCE* sequence showing deformation effect, augmentation cues omitted.

Similarly, augmentation cues should pass behind occluding objects. Fortunately these cues traverse an identical path to that of the feature in prior frames. We construct an *occlusion buffer* over time, summing the difference images generated whilst handling occlusion for deformation cues (Fig. 9D). Using this buffer we may determine which pixels will occlude the streak lines, so long as those pixels do not change in the time interval between the feature passing and the augmentation cues being drawn. The occlusion buffer contains a difference image for occlusion and the RGB value of each pixel. Pixels in the buffer are deleted when the difference between the stored colour for a pixel, and the measured colour of that pixel at the current time is significant. In this case the occluding pixel has moved, obsoleting our knowledge of it. This algorithm works acceptably well over short time intervals (Fig. 9E).

4.4. Compositing and rendering

We generate a background for each video frame by subtracting features from the original video; determining which pixels in the original video constitute features by projecting tracked feature regions from the camera-compensated sequence to the original viewpoint. Pixels contributing to feature regions are deleted and absent background texture is reprojected from locally neighbouring frames in alternation until holes are filled with non-feature texture. This sampling strategy mitigates against artifacts caused by local lighting changes or movement.

Once augmentation and deformation cells have been rendered for each feature, cells are composited to produce an output video frame. Cells are projected by homography to coincide with the original camera viewpoint, and composited onto the background in reverse depth order. Thus motion cues appear to be inserted into video at the correct scene depth (Fig. 9G). Additionally, temporally coherent NPR shading effects may be generated by rigidly attaching strokes or texture to each feature; strokes are subjected to the identical LCAT motion and deformations as their respective feature (Fig. 9F).

5. Conclusion and discussion

We have described and demonstrated a system for the artistic rendering of motion within video sequences. The system can cope with a moving camera, lighting changes, and presence of occlusion. Users may stylise both the placement and appearance of motion cues using the parameterised framework described in Section 4. Novel effects may be produced by interpolating between points in this parameter space, gradually changing the appearance of motion cues over time.

Further developments could address the relaxation of some of the assumptions made in the design of the system. For example, violations of depth assumptions are detectable by the presence of heavily weighted cycles in the depth graph. It may be possible to segment video into a minimal number of chunks exhibiting non-cyclic depth graphs, and in doing so recover relative feature depth under more general motion. The robustness of the algorithm could be evaluated both with ground truth comparisons for measures such as velocity, as well as processing sequences exhibiting distinctly non-planar motion. We might also extend the possible gamut of motion cues; investigating whether additional techniques in Lasseter's paper [5] such as anticipation, can be rendered automatically.

We briefly described a means of coherently shading the animation by applying strokes or adaptive texture (such as Q-maps) to cells. Coherence is maintained so long as the LCAT-derived motion of cells matches the perceived motion of content within them; in cases of movement within the background cell some deterioration in temporal coherence may be observed. Current work focuses upon extending our system to incorporate our recently proposed "Stroke Surfaces" NPR video framework [17]. Briefly, background and deformation cue cells are buffered prior to output yielding a set of spatio-temporal voxel volumes, with time as the third dimension. The stroke surface rendering framework is then applied to these volumes to generate a variety of coherent stylised shading effects in tandem with the motion cues generated by our system.

We have shown that through high-level analysis of features (examining motion over the entire video, rather than on a per frame basis) we may produce motion cues closely approximating those used in traditional animation (Fig. 1). We believe the most productive avenues for future research will not be in incremental refinements to the current system, but rather will examine alternative uses for higher-level spatio-temporal analysis of video with applications to NPR.

A selection of rendered video sequences, and further details of the Video Paintbox project, are available on-line at: http://www.cs.bath.ac.uk/~vision/cartoon.

References

[1] B. Meier, Painterly rendering for animation, in: Proceedings Computer Graphics (ACM SIGGRAPH), 1996, pp. 447–484.
[2] E. Daniels, Deep canvas in disney's tarzan, in: Proceedings Computer Graphics (ACM SIGGRAPH, Abstracts and Applications), 1999, p. 200.
[3] P. Litwinowicz, Processing images and video for an impressionist effect, in: Proceedings Computer Graphics (ACM SIGGRAPH), Los Angeles, USA, 1997, pp. 407–414.
[4] A. Hertzmann, K. Perlin, Painterly rendering for video and interaction, in: Proceedings NPAR Symposium, 2000, pp. 7–12.
[5] J. Lasseter, Principles of traditional animation applied to 3D computer animation, in: Proceedings Computer Graphics (ACM SIGGRAPH), vol. 21, 1987, pp. 35–44.
[6] S. Chenney, M. Pingel, R. Iverson, M. Szymanski, Simulating cartoon style animation, in: Proceedings NPAR Symposium, 2002.
[7] T. Strothotte, B. Preim, A. Raab, J. Schumann, D.R. Forsey, How to render frames and influence people, in: Proceedings Computer Graphics Forum (Eurographics), vol. 13, Oslo, Norway, 1994, pp. C455–C466.
[8] S.C. Hsu, I.H.H. Lee, Drawing and animation using skeletal strokes, in: Proceedings Computer Graphics (ACM SIGGRAPH), 1994, pp. 109–118.
[9] J.P. Collomosse, P.M. Hall, Cubist style rendering from photographs, IEEE Trans. Vis. Computer Graph. 4 (9) (2003) 443–453.
[10] P.H.S. Torr, Motion segmentation and outlier detection, Ph.D. thesis, University of Oxford, 1995.
[11] C.J. Harris, M. Stephens, A combined corner and edge detector, in: Proceedings 4th Alvey Vision Conference, Manchester, 1988, pp. 147–151.
[12] M.A. Fischler, R.C. Bolles, Random sample consensus: a paradigm for model fitting with applications to image analysis and automated cartography, Commun. ACM 24 (6) (1981) 381–395.
[13] R. Szeliski, Image mosaicing for tele-reality applications, Tech. rep., Digital Equipment Corporation, 1994.
[14] D. Williams, M. Shah, A fast algorithm for active contours and curvature estimation, CVGIP: Image Understanding 55 (1) (1992) 14–26.
[15] A.W. Fitzgibbon, R.B. Fisher, A buyer's guide to conic fitting, in: Proceedings BMVC, Birmingham, 1995.
[16] P. Hall, Non-photorealistic rendering by Q-mapping, Computer Graphics Forum 1 (18) (1999) 27–39.
[17] J.P. Collomosse, D. Rowntree, P.M. Hall, Stroke surfaces: A spatio-temporal framework for temporally coherent non-photorealistic animations, Tech. Rep. 2003–01, University of Bath, UK (June 2003).